Emerging Strategies toward Mechanically Robust Organic Photovoltaics: Focus on Active Layer

Cenqi Yan, Jiaqiang Qin, Yinghan Wang, Gang Li and Pei Cheng**

[*] Dr. C. Yan, Prof. J. Qin, Prof. Y. Wang, Prof. P. Cheng

College of Polymer Science and Engineering, State Key Laboratory of Polymer Materials Engineering, Sichuan University, Chengdu 610065, China

Email: chengpei@scu.edu.cn

[*] Dr. C. Yan, Prof. G. Li

Department of Electronic and Information Engineering, Research Institute for Smart Energy (RISE), The Hong Kong Polytechnic University, Hung Hom, Kowloon, Hong Kong, China

Email: gang.w.li@polyu.edu.hk

Keywords: mechanically robust, mechanically durable, stability, organic photovoltaics, active layer

Abstract

Mechanical stability of organic photovoltaics (OPVs) is required not just for portable applications, which must accommodate strain as a function of operation, but also for manufacturing, transportation, and utility-scale applications. However, the mechanical reliability of OPVs is often disregarded compared with other stress (thermal, oxygen, moisture, irradiation). The key to improving the mechanical stability of OPVs lies in realizing mechanically robust active layer. This perspective first analyzes working scenarios of flexible OPVs (static and dynamic conditions) and strategies towards mechanically robust active layer. Then, the recent achievements in improving the mechanical robustness of active layers are summarized in the aspects of all-polymer active layers, single-component active layers, and third component strategy. In the end, outlook and perspective are provided to improve the mechanical stability of active layers.

1. Introduction

Organic photovoltaics (OPVs) are seen as promising power generation technology that can be incorporated into flexible and portable electronics, due to their benefits, such as low carbon footprint, low-temperature manufacturing, and ease of fabrication into flexible and lightweight devices.[1-10] Recent advancements in materials design, device engineering, and device physics have resulted in a significant improvement in power conversion efficiencies (PCEs) of OPVs, with values presently above 20%, meeting the commercialization efficiency criterion.[11-14] Despite the commercially viable PCE, the stability of OPVs remains a major concern. Oxygen, moisture, irradiation, thermal, and mechanical stress are factors that restrict the stability of OPVs. In the past decades, these oxygen-, moisture-, irradiation-, and thermal stabilities have been extensively studied to meet commercial applications.[15-20]

The biggest advantages of OPV to complement with inorganic photovoltaics in the future lie in the flexibility of organic active-layer materials, which not only enables the roll-to-roll processing[21] but also allows the integration of OPV devices in many form factors inaccessible by inorganic devices, such as clothing, portable electronics, agricultural greenhouses, biomedical applications, and extremely flexible and stretchable devices.[22-33] For instance, Someya et al.[34, 35] demonstrated washable, stretchable, and lightweight OPVs with a PCE of 7.9% as textile-compatible power

sources, which can be used as a long-term power source for wearables, electronic textiles as well as sensors for the Internet of Things. Mechanical stability is required not only for the portable applications mentioned above, which must accommodate strain as a function of operation, but also enable the solar module to withstand the impact, vibration, and other stresses that occur during manufacturing, transportation, and utility-scale applications. For example, to withstand different sorts of mechanical stresses during the coating process (e.g. roll-to-roll printing), a consistent degree of stretchability and flexibility is necessary. Furthermore, steady performance under constant mechanical stress should be ensured to meet the real-world applications of portable and wearable devices. However, the mechanical reliability of OPVs has received far less attention than other aspects of stress and is far from adequate for commercial application.

Conjugated polymers for the OPV active layer have intrinsic mechanical deformability, which sets them apart from their inorganic counterparts. The upper limit of PCE and mechanical stability of the overall OPV device would be determined by an appropriate active layer with optimized morphology. In fact, the active-layer system of the state-of-the-art OPVs with PCEs of ~20% can hardly meet the demands of flexible electronics. Recently, there has been a growing awareness of the importance of mechanical robustness; scientists have reported a variety of conceptual research aimed

at mechanically reliable OPVs, making it a hot issue in the field of OPVs.

This perspective first classifies the working scenarios of flexible OPVs: static condition (low-frequency large deformations) and dynamic condition (high-frequency small deformations), and then discusses the corresponding strategies towards mechanically robust active layer: improve ductility, strengthen phase stability, and restrain molecule migration. Afterward, the current achievements in improving the mechanical robustness of active layers are summarized in the aspects of all-polymer active layers, single-component active layers, and third component strategy. The third component can be insulating polymers, reactive small molecules, donor/acceptor (D/A) compatibilizers, polymer donor/acceptor, fullerenes, etc. In the end, the outlook and challenges of mechanically stable OPVs are presented.

2. Parameters of mechanical properties and Related Characterization

The stress-strain curve of material provides the information of the stress-strain relationship (Scheme 1). The first stage is the linear elastic region, where the stress is proportional to the strain. It obeys the general Hooke's law and the slope is Young's modulus. The yield point is the point on a stress-strain curve that indicates the end of elastic region and the beginning of plastic region. The yield stress/strength and yield strain refer to the stress and strain corresponding to the yield point, respectively. Crack onset strain refers to the strain when fracture starts to appear. Cohesive fracture energy,

G_c, is indicative of the work required to produce a new cracked surface per unit area during the fracture of the material. Tensile strength, which is short for ultimate tensile strength, is the maximum stress that a material can withstand while being stretched or pulled before breaking. Toughness is the amount of energy per unit volume that a material can absorb before fracture.

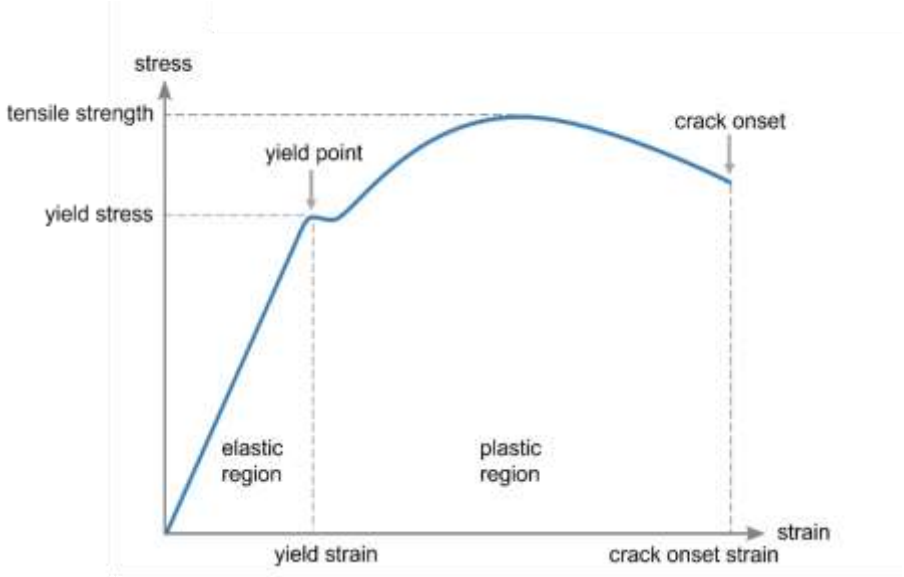

Scheme 1. The hypothetical stress-strain curve.

There are mainly four methods to investigate the mechanical properties of active layers: Bucking Metrology, Film-on-Elastomer, Nanomechanical Mapping, and Film-on-Water. Buckling Metrology on soft elastomeric substrates exploits the formation of surface wrinkles to estimate the elastic modulus of a film deposited on a softer elastomeric substrate. Film-on-Elastomer is one of the most widely used techniques to investigate the mechanical properties, especially for the crack-onset strain (COS) and

yield point. A thin film of material is directly laminated onto a soft elastomer, through direct contact lamination, or film floating on water. The resulting polymer thin Film-on-Elastomer can be directly stretched to different strain values and geometry, thus allowing for a precise and in-depth investigation of mechanical properties. Similar to the Film-on-Elastomer technique, the Film-on-Water method can measure elastic modulus, COS, and yield point. This tool relies on the direct stretching of freestanding films suspended on water rather than being supported on an elastomeric substrate, which can minimize the influence of the substrate. Nanomechanical Mapping, directly measures the mechanical properties of thin film by analyzing tip-sample interaction forces through a soft and non-destructive indentation. It can obtain topographic high-resolution information to evaluate COS, and local material properties such as the elastic modulus, adhesion, and stiffness.

3. Working scenarios and strategies towards mechanically robust active layer

Before discussing the mechanical robustness of active layer, we should classify the main working conditions into two kinds: static condition (low-frequency large deformations) and dynamic condition (high-frequency small deformations). The static condition means that there exists a large extent of deformation in low-frequency. For example, in the roll-to-roll printing process, the active layer undergoes a large extent of deformation of short duration. The dynamic condition means that the product is

subjected to a large number of alternating loads with small deformations; in another word, OPVs are frequently stretched and curled to a slight degree. For instance, when OPVs are integrated into wearable devices, they are exposed to multiple strain cycles. Strategies towards mechanically robust active layer may differ with work scenarios and requirements.

Strain applied to active layer can induce change in chain alignment, texture and crystallinity.[22] At a larger length scale, strain may influence D/A phase separation and induce cracks. The well-known effect of tensile strain on a conjugated polymer is chain alignment along the strained axis, which accounts for the exceptionally high tensile strength of uniaxially aligned polyacetylene.[36] A secondary effect is texture. For instance, O'Connor et al.[37] found that strain induced a significant face-on orientation in the film originally with highly edge-on orientation. The third effect is crystallinity. For instance, P3HT under strain exhibits stronger crystallinity, evidenced by the increased intensities of the vibronic transitions. The nanometer-sized domains can slide against each other to accommodate large external deformations. Beach sand is a natural analog for the nanograin morphology. The grains can slide against each other whether the sand is dry or submerged in water.[38] Strain can induce thin areas and even cracks in active layer, which produce shunts and reduce parallel resistance, and therefore decrease fill factor (FF) and open-circuit voltage (V_{OC}).

Strategies towards mechanically robust active layer are shared in Figure 1 and discussed in term of improve ductility, strengthen D/A interfaces and restrain molecule migration.

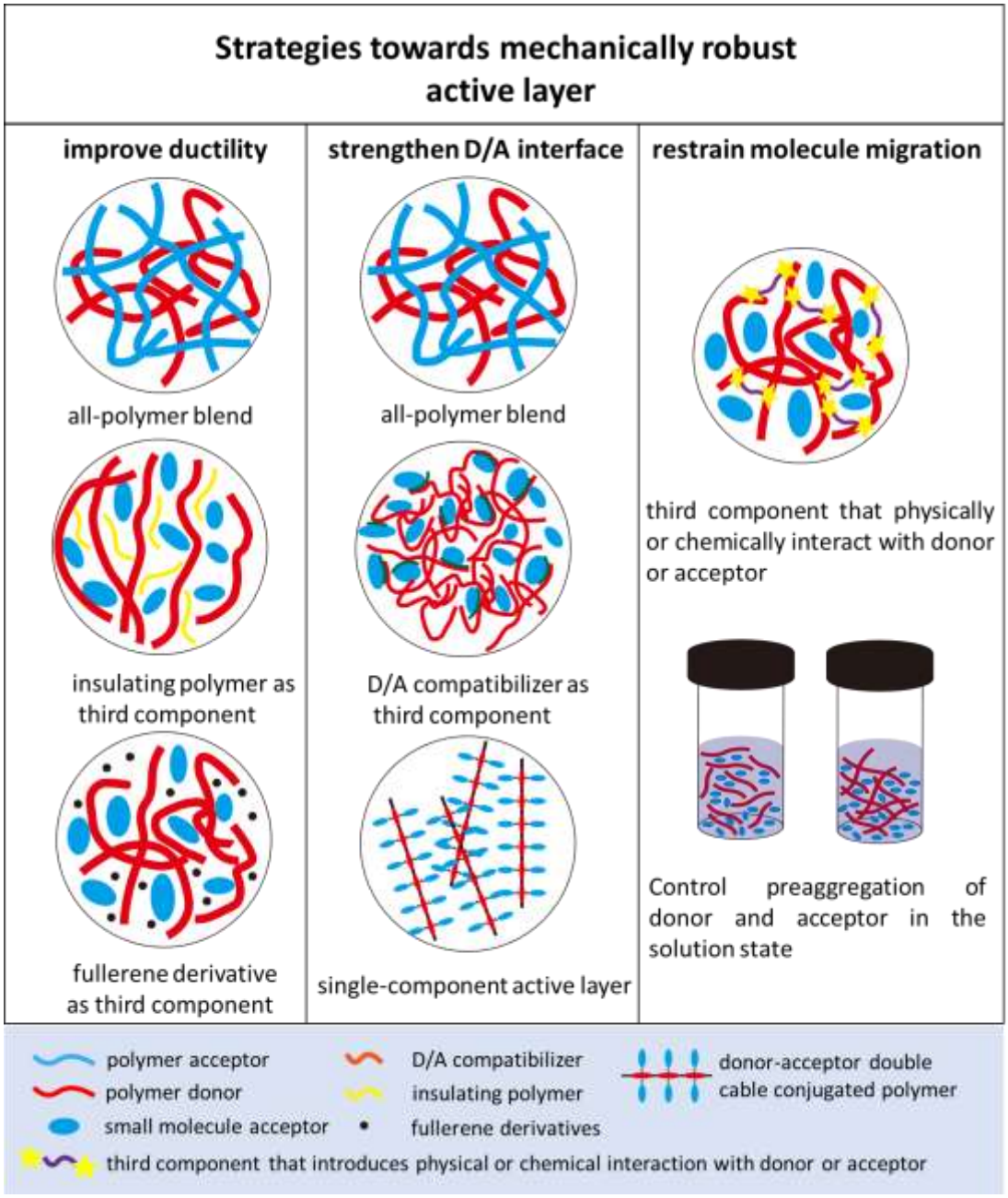

Figure 1. Scheme of strategies towards mechanically robust active layer. The first strategy is to improve ductility. Example includes constructing all-polymer blend, introducing insulating elastic polymer and fullerene derivatives as the third component.

The second one is strengthening D/A interfaces. Examples include constructing all-polymer blend, introducing D/A compatibilizer as third component, or using single-component active layer. The last is to restrain molecule. Examples include using third component that physically or chemically interact with donor or acceptor, and controlling materials' preaggregation in the solution state.

A. Improve ductility. Ductility means the ability of a material to have its shape changed without losing strength or breaking. The ductility of active layer can be improved from materials and structures. 1) Polymer donors and acceptors are typically more ductile than small molecules, making an all-polymer system a viable choice. The rational chemical design of flexible π-conjugated backbone and side chains and large molecular weight (MW) can improve stretchability and COS. The design of block copolymers containing conjugated blocks linked to soft coil segments is also effective in improving mechanical property.[39] Flexible thermoplastic elastomers, insulating polymers and resins, and other materials with high ductility can be incorporated to increase the ductility of active layer. Reactive small-molecule additives that crosslink to create an internal elastic network after deposition are also viable. 2) Balance the ratio of amorphous and ordered molecular aggregations that coexist in the domains of active layer. Amorphous regions can dissipate loading stress by altering coil conformations,

which plays a crucial role in the stretchability of overall active layer. Ordered packing is generally stiff, and grain boundaries scattered in active layer may become weak spots under strain, potentially resulting in fractures and cracks.

B. Strengthen D/A interfaces. The sharp and weak D/A interfaces are at a high risk for the occurrence of debonding cracks, resulting in low cohesion and mechanical fragility.[40] 1) The presence of substantial tie molecules and entangled chain networks form strengthened D/A interfaces within the active layer films and brings about a high concentration of amorphous regions, which reduce fracture propagation channels. The finely separated morphology without large aggregates in all-polymer blend can alleviate the stress concentration at the D/A interfaces and thereby inhibit the decohesion. 2) Pure active layer based on double-cable conjugated polymers can exhibit excellent mechanical property by eliminating phase stability issues. Compared with binary-component active layer, neat double-cable polymer film is more inclined to remain unchanged under mechanical stimuli.[41] 3) A D/A compatibilizer can reduce the interfacial tension between donor-acceptor phases, which can engender larger interface with increased mixed domain, improve interfacial adhesion/cohesion properties within the donor-acceptor heterojunctions, and suppress excessive coalescence of domains via the formation of kinetic barriers.[42]

C. Restrain molecule migration. Cross-linkable donors/acceptors can be utilized, and

a third component can be introduced to reinforce the donor or acceptor network via physical/chemical interactions. The preaggregation of donor/acceptor materials in the solution can be controlled to strengthen the donor or acceptor network in active layer.

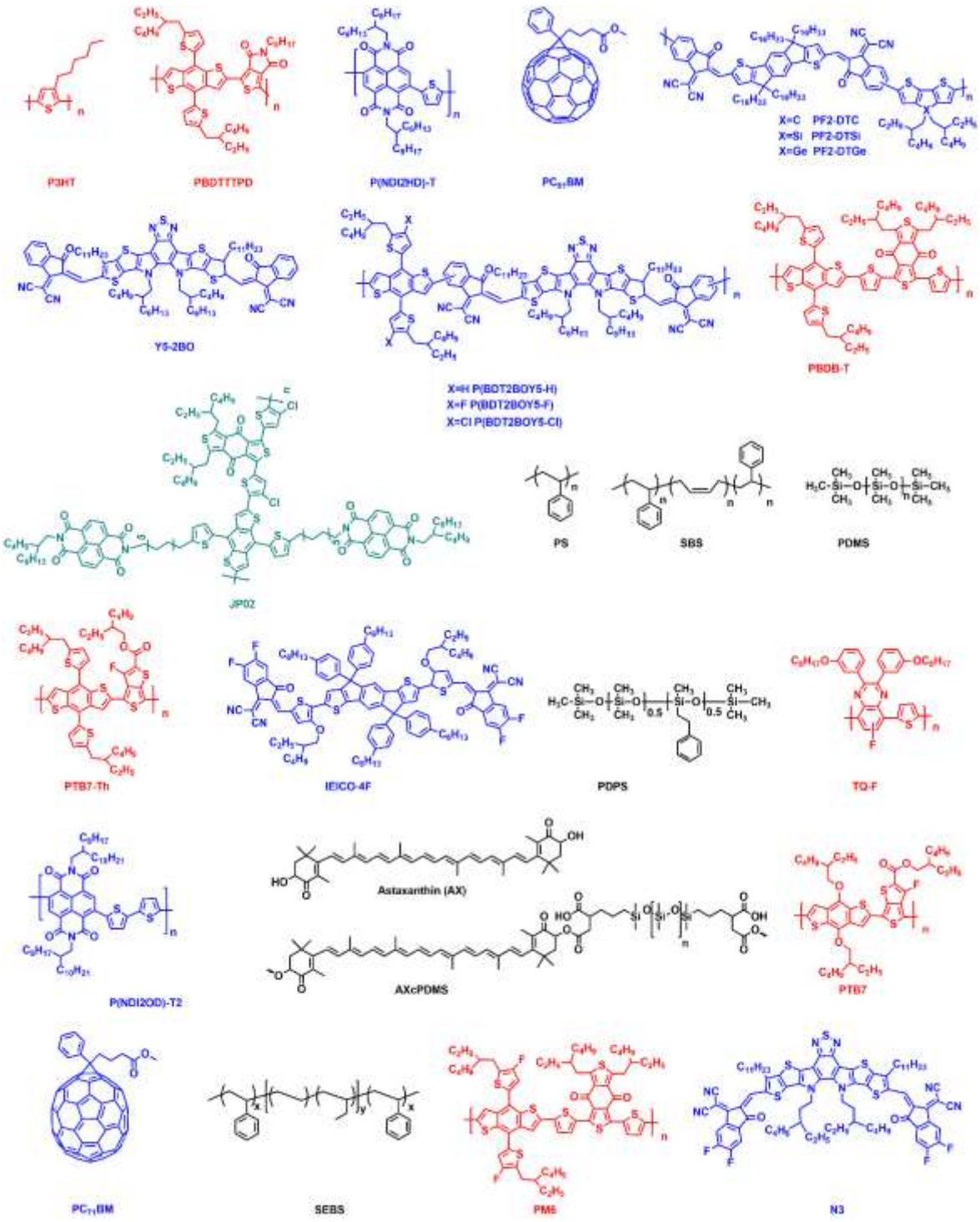

Figure 2-1. Chemical structures of materials discussed in this manuscript. Donors are

depicted in red, acceptors are depicted in blue, donor-acceptor double cable conjugated polymer is depicted in green, and the third components are depicted in black.

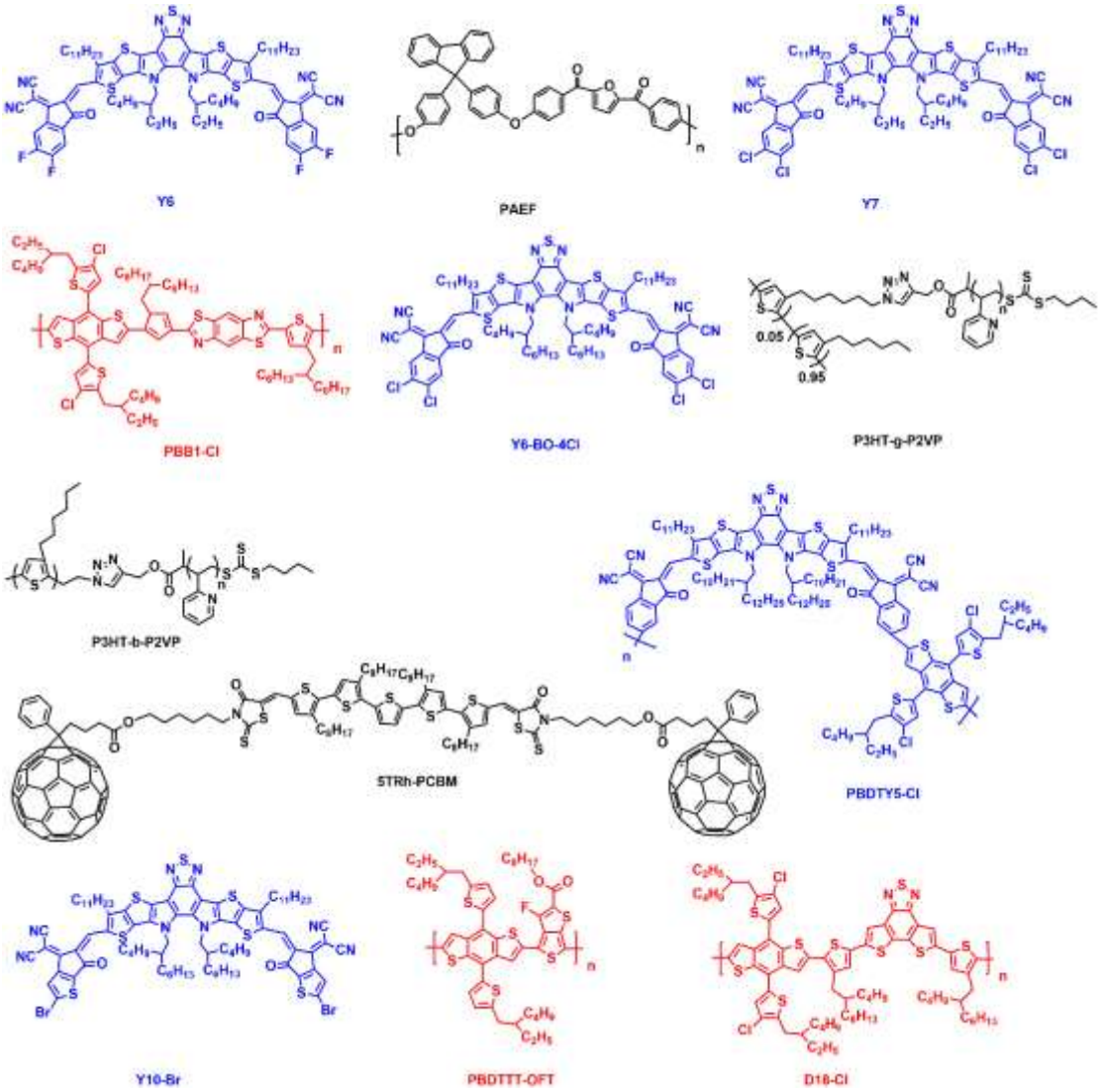

Figure 2-2. Chemical structures of materials discussed in this manuscript. Donors are depicted in red, acceptors are depicted in blue, donor-acceptor double cable conjugated polymer is depicted in green, and the third components are depicted in black.

4. Methods toward mechanically robust active layer

4.1. All-polymer active layer

As aforementioned, improving molecular aggregation and mechanical reliability simultaneously is rather paradoxical for OPVs based on small-molecule acceptors (SMAs). All-polymer systems are recognized for good mechanical, thermal- and irradiation stability.[40, 43-47] Stretchability is typically better in all-polymer blend films than small-molecule films. Polymer acceptors are intrinsically more ductile than SMAs. All-polymer active layer can form better entanglements between the polymer chains, both within domains and at D/A interfaces. A large plastic conformation and flexible polymer bridging chains conduce to a large plastic zone at the crack tip during crack growth in all-polymer active layer.

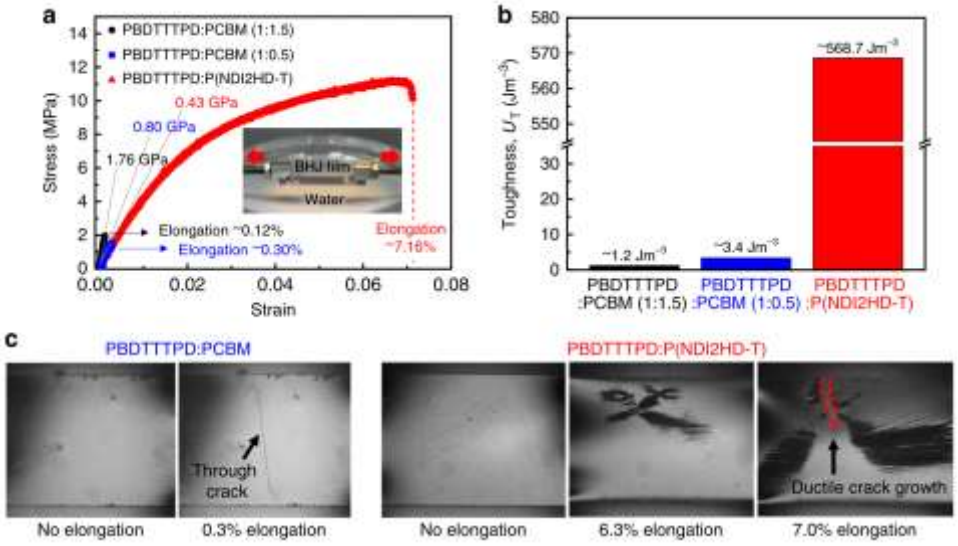

Figure 3. Tensile test of PBDTTTPD: $PC_{61}BM$ and PBDTTTPD: P(NDI2HD-T) blend films. (a) Strain–stress curves and (b) toughness of PBDTTTPD: $PC_{61}BM$ and

PBDTTTPD: P(NDI2HD-T) blend films. (The inset shows photographs of active layer floating on water. The specimens were gripped by the PDMS-coated Al grips and the films were prepared under the optimized device condition). (c) Optical microscopy images of PBDTTTPD: $PC_{61}BM$ (1:0.5 w/w) and PBDTTTPD: P(NDI2HD-T) (1.3:1 w/w) blend films when the films were under different strains. Reproduced under the terms of a Creative Commons Attribution 4.0 International License.[48] Copyright 2015, The Authors.

Kim et al.[48] developed mechanically robust OPVs based on the PBDTTTPD: P(NDI2HD-T) all-polymer system, which exhibited a higher PCE of 6.64% than the PBDTTTPD: $PC_{61}BM$ control (6.12%).(**Figure 2** depicts chemical structures of representative donors, acceptors, double-cable conjugated polymer, and additives listed in this manuscript and Table1 summarizes mechanical properties of active layers and related device performance of OPVs.) More importantly, under the static condition, all-polymer OPVs dramatically outperformed the fullerene devices in strength and flexibility, with elongations at break increasing from 0.30% to 7.16% and toughness increasing from 3.4 to 568.7 J m^{-3}, respectively (**Figure 3**). They further found that with increasing molecular weight above the entanglement threshold, the corresponding materials can form tie molecules and chain entanglement, interconnect adjacent

domains, and therefore effectively transfer load to neighboring chains, which significantly increased the COS, ductility, and toughness of active layer.[49] Meanwhile, the increase of molecular weight also improved short-circuit current density (J_{SC}) and PCE.

However, all-polymer OPVs typically exhibit lower PCE than their counterparts based on nonfullerene SMAs, owing to the low extinction coefficients (≈0.3–0.4 × 10^5 cm^{-1}) and charge mobilities (≈10^{-5} cm^2 V^{-1} s^{-1}) of polymer acceptors based on perylene/naphthalene diimide (PDI/NDI) moieties.[50] By polymerizing moieties of nonfullerene SMAs, novel polymer acceptors with strong light absorption and high charge mobilities have been constructed.[51] Wang et al.[52] designed three narrow bandgap polymer acceptors with different bridging atoms (PF2-DTX, X= C, Si, and Ge). The corresponding neat films exhibited monotonically decreased elongation at break (from 31.7% to 14.6% and 5.9%), tensile strength (from 24.9 to 20.5 and 17.5 MPa), elastic modulus (from 1.06 to 0.93 and 0.67 GPa), and integrated toughness from 6.61 to 2.50 and 0.83 MJ m^{-3}, with the increased mass of the bridging atom. The active layer bearing PF2-DTSi demonstrated the highest PCE of 10.77% due to better charge separation and transport, and optimized morphology, as well as excellent mechanical resilience, with toughness of 9.3 MJ m^{-3} and an elongation at break of 8.6%. Consequently, after bending and relaxing 1,200 times at a bending radius of 4 mm, the

flexible all-polymer OPVs bearing PF2-DTSi preserved > 90% of its original PCE.

The D/A interfaces with small area and narrow width, caused by the incompatibility between polymer donors and acceptors, impair PCE, morphological stability, and mechanical robustness. Designing polymer acceptors that contain the same building block as polymer donors is an effective approach to increasing D/A compatibility. Kim et al.[53] reported the co-polymerization of Y5-2BO nonfullerene SMA with benzodithiophene (BDT) moieties to produce a series of nonfullerene SMA-based polymer acceptors [P(BDT2BOY5-X), X=H, F, Cl]. Because of the shared BDT unit, PBDB-T: P(BDT2BOY5-X) blends had better molecular compatibility and a lower $\gamma_{D\text{-}A}$ value of 0.3–0.4 mN m^{-1} than PBDB-T: P(NDI2OD-T2) (1.64 mN m^{-1}) and PBDT-T: Y5-2BO (2.21 mN m^{-1}). All-polymer OPVs based on PBDB-T: P(BDT2BOY5-X) blends exhibited a higher PCE of 11.12% than those based on P(NDI2OD-T2) (6.00%) and Y5-2BO (7.02%). The mechanical characteristics were also significantly enhanced with the PBDB-T: P(BDT2BOY5-Cl) blend, exhibiting a sevenfold increase in COS (15.89%) and a tenfold increase in toughness (3.24 MJ m^{-3}) compared to the PBDB-T: Y5-2BO blend (COS of 2.21% and toughness of 0.32 MJ m^{-3}). The higher ductility of the PBDB-T: P(BDT2BOY5-X) blend was mostly ascribed to increased acceptor backbone length due to polymerization and improved D/A miscibility. Long polymer acceptor chains that interacted with each other and generate

tie molecules that bridged neighboring crystalline domains and the well-intermixed domains are both effective in dissipating stress.

4.2. Single-component active layer

Single-component OPVs are based on ambivalent materials containing both electron donor and acceptor units capable of ensuring the functions of light absorption, exciton dissociation, and charge transport. Compared with bicomponent and multicomponent OPVs, single-component OPVs present major advantages of simplified fabrication stabilized D/A interface and long device lifetime.[54] Brabec et al.[55] demonstrated that single-component OPVs using double-cable conjugated polymers as active-layer materials exhibited outstanding thermal and irradiation stability. Importantly, by removing phase separation concerns, single-component OPVs with a pure polymer photoactive layer can function with good mechanical robustness, revealing its promising potential in flexible OPVs.

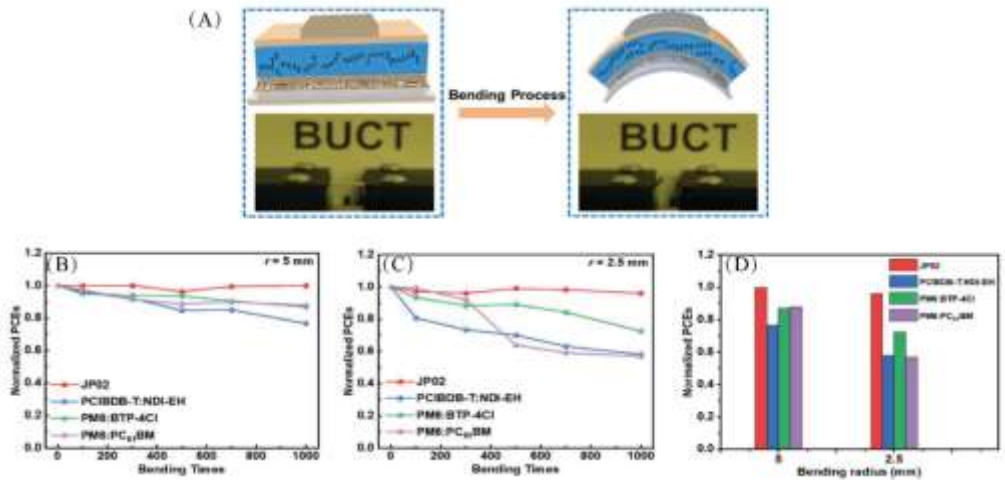

Figure 4. Mechanical durability of flexible OPVs. A) Schematic diagram and optical images of the mechanical bending process. The normalized PCEs changes of the flexible single-component OPVs and BHJ-type OPVs with different bending cycles at bending radius B) r = 5 mm and C) r = 2.5 mm. D) The normalized PCEs changes of the flexible single-component OPVs and different BHJ-type OPVs with 1000 bending cycles at different bending radii. Adapted with permission.[41] Copyright 2021, Wiley-VCH.

Li et al.[56-59] inserted NDI units into double-cable polymers, and adjusted the miscibility between conjugated backbones and side units by changing the position of Cl atoms. The miscibility of the segments in JP02 was improved when Cl atoms were positioned at the major chains, which contributed to exciton diffusion and dissociation. Therefore, JP02-based SCOSCs achieved a high PCE of 8.40%. They[41] constructed a flexible single-component OPV using a double-cable conjugated polymer JP02 (**Figure 4**). The flexible single-component OPVs displayed PCEs of 7.21% compared to those of the rigid devices (8.02%). The active layer based on JP02 had good mechanical qualities. After 1000 bending cycles at bending radii ranging from 7 to 2.5 mm, the flexible single-component OPVs retained >95% of their initial PCEs. They further introduced three different insulating polymers (PS, styrenebutylene-styrene (SBS), and

PDMS) into JP02 thin films.[60] The measured miscibility order was JP02-PDMS < JP02-SBS < JP02-PS. The optimal blends of JP02-PS with the best miscibility exhibited COS of up to 4.69% and the corresponding PCE of 6.71% in relative to the neat JP02 film with COS of 2.48% and PCE of 7.51%, while the PCEs reduced to 5.93 and 5.96% along with lower COS in JP02-PDMS and JP02-SBS systems, respectively. In term of using insulating polymers, miscibility is a critical factor to balance photovoltaic performances and mechanical properties. The better miscibility allows for more favorable interfacial contacts at the amorphous phase, which can enhance their mechanical robustness and maintain charge-transport pathway simultaneously.

4.3. Ternary component strategy

4.3.1. Insulating polymers

Recently, the addition of insulating polymers as the third component has been recognized as a facile strategy to improve mechanical robustness. Polydimethylsiloxane (PDMS), employed as a lubricant in syringes to distribute polymer "inks" for spin-coating, is effective in optimizing morphology and PCE in all-small-molecule solar cells. Moreover, the use of PDMS and its derivatives is highly beneficial for improving mechanical stability. Shao et al.[61] devised a transfer printing approach, in which D-sorbitol was introduced into the PEDOT:PSS PH1000 hole transport layer (HTL) to improve adhesion with the PTB7-Th: IEICO-4F active layer. The COS of PTB7-Th:

IEICO-4F active layer increased from 5% to 20% with the incorporation of 5% PDMS plasticizer. The plasticizing effect of PDMS, which increased the free volume between polymer chains in bulk heterojunctions, weakened polymer interchain interaction, and facilitated polymer chain movement under external strain, was considered as the source of the increased ductility. The deposition of high-quality active layer on the stretchable substrate is enabled by this transfer printing technology, resulting in a PCE of 10.1%. The stretchable OPVs demonstrate ultra-flexibility, stretchability, and mechanical robustness, which make the PCE almost unaffected after 300 bending cycles with a bending radius of 2 mm. Meanwhile, the device retains 86.7% PCE under tensile strain as large as 20%. By grafting styrene to the PDMS backbone, Yang et al.[62] designed a high-viscosity hydrophobic PDPS with a fourfold increase in viscosity as an additive in TQ-F: N2200-based all-polymer OPVs. A robust intercalated phase-separated network with desirably-controlled nanocrystallite sizes was observed in the active layer with 10% PDPS. This film has a comparable tensile strength of 24.62 MPa (24.97 MPa for 0% PDPS), a lower elastic modulus of 0.54 GPa (0.75 GPa for 0% PDPS), a much higher elongation at break of 50.92% (32.56% for 0% PDPS), and thus a higher toughness value of 9.67 MJ m^{-3} (6.90 MJ m^{-3} for 0% PDPS). The storage (G') and loss (G'') moduli of active layer exhibit a weak dependence on the frequency, where the G' values were higher than those of the corresponding G'' over the measured frequency

range, indicating typical gel-type behavior. The G′ and *G″* moduli grow with the increased PDPS concentration. Further increase of the PDPS content results in a monotonic decrease in elastic modulus and tensile strength. And the elongations at break in active layers with 20% PDPS and 50% PDPS are 53.15% and 42.96%, respectively. They made a graphene electrode-based flexible device using the best-performing blend with 10% PDPS, which has a high PCE of 5.60 % and retains 90% of its original PCE after 100 bending cycles with a 3.0-mm bending radius.

Madsen et al.[63] used a combination of plasticizers and antioxidants to enhance mechanical stability. They designed AXcPDMs, a novel covalent combination of antioxidant astaxanthin (AX) with PDMS. 3wt% AX reduced the elastic modulus of the PTB7:$PC_{71}BM$ film from 2.19 to 1.27 GPa, presumably because the preferred interaction of AX with $PC_{71}BM$ disturbs the formation of PTB7 pure crystalline phases. Upon the addition of 1.5 wt% PDMS, the tensile modulus of the corresponding films (1.98 GPa) remained comparable to the reference, presumably ascribed to the poor miscibility of PDMS with PTB7 and $PC_{71}BM$. With the addition of 1.5 wt% PDMS and 3 wt% AX, a comparable tensile modulus of 2.36 GPa was observed, where the beneficial impact of AX intercalating into $PC_{71}BM$ was hindered by PDMS. The elastic modulus was lowered to 1.36 GPa with AXcPDMS, ascribed to the enhanced miscibility between PDMS and the active layer due to the presence of AX grafted to

PDMS.

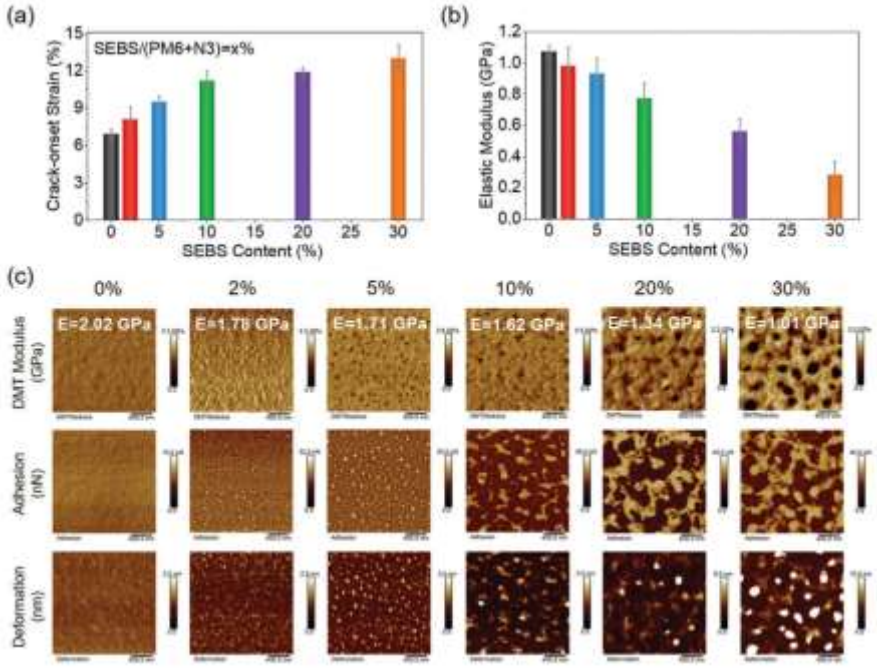

Figure 5. a) Crack-onset strain and b) elastic modulus of the PM6:N3:SEBS ternary blend films measured by film-on-elastomer (FOE) method. c) Derjaguin-Muller-Toporov (DMT) modulus, adhesion, and deformation images of the PM6:N3:SEBS blend films with varying SEBS content obtained by the peak force quantitative nanomechanical mapping (PFQNM) method. The modulus data indicated in the DMT modulus images are average values. Reproduced with permission.[64] Copyright 2021, Wiley-VCH.

By inducing polystyrene-block-poly(ethyleneran-butylene)-block-polystyrene (SEBS), Ye et al.[64] successfully increased the stretchability and lowered the stiffness of the PM6:N3 active layer while maintaining high PCE (**Figure 5**). SEBS, as a

commercial insulating thermoplastic elastomer, has exceptional ductility with a COS of 1050%, two orders of magnitude greater than PM6, and an elastic modulus of 1.3 MPa, two to three orders of magnitude lower than conventional conjugated polymers. The PM6:N3 active layer was brittle and stiff, with a COS of merely 7% and an elastic modulus of the order of 1 GPa, severely restricting its use in stretchable electronics. The COS of ternary blend films steadily increased with the increased SEBS ratio, and the elastic modulus and fracture size dropped monotonically. The SEBS phase was isolated and tiny at a low content of 2%, and the stretchability improvement was attributed to more soft/ductile aid (small SEBS phases), better out-of-plane packing, and a larger face-on proportion. At a content of 5wt%, stretchability was improved due to an increase in the soft/ductile SEBS and better out-of-plane packing. At a content of >10 wt%, the large and interconnected SEBS domain was primarily responsible for the enhancement of stretchability, which prevented the chain-sliding effect of the polymer donor/SMA in the blend films. With 30 wt% SEBS, the COS was improved by a factor of ≈2 and the elastic modulus dropped to ≈1/4. The addition of < 5 wt% SEBS slightly improved PCE from 15.4% to 16%.

Poly(aryl ether) (PAE) is high-temperature-resistant polymer successfully employed to construct high-performance composite materials and high-modulus fibers. The main chain of PAE is extensively twisted to promote solubility in organic solvents,

while stiff aromatic backbones without soft side chains provide outstanding thermal stability, large tensile strength, and high elongation at break. Chu et al.[65-67] introduced insulating PAE matrices to OPVs. The devices based on PM6/Y6 with 5 wt% PAEF resin exhibited a higher PCE (16.13%) than the unprocessed one (15.44%). The device bearing 30 wt% PAEF still shows a high PCE of 15.17%. The active layer with 30 wt% PAEF displayed a remarkable 4.4-fold strain of 25.07% compared with the PM6:Y6 film (5.75%). PAEF matrices showed tunneling effects without changing charge transport channels, introduced strong chain entanglement effect, restrained the migration of molecular chains, and fasten the active-layer morphology.

4.3.2. Reactive small molecules

Compared with polymer additives, reactive small molecules more readily blend with donor and acceptor and can be cross-linked after casting in the active layer.

Verduzco et al.[68] improved the mechanical stability of active layers by incorporating an internal elastic network. Network-stabilized OPVs were fabricated using reactive small molecular additives that were rapidly cross-linked through thiol−ene coupling. Thiol−ene reactions catalyzed by a base or initiated through short exposure to UV irradiation produced insoluble, elastic thiol−ene networks in the active layer. The addition of up to 20 wt% reactive small molecules did not impair PCE and significantly increased COS from 6% to 26%.

4.3.3. polymer acceptor or donor

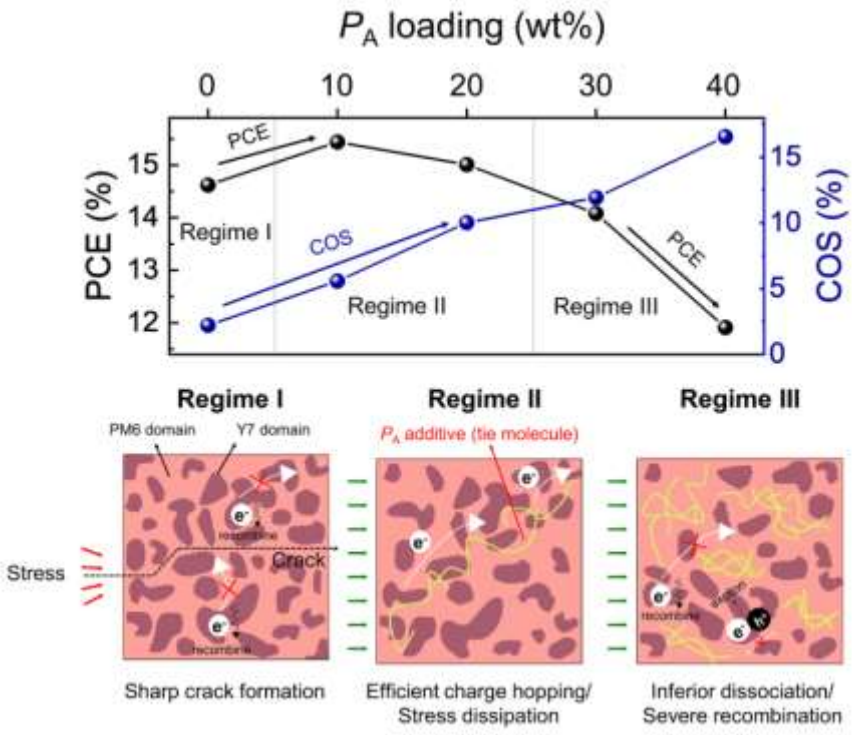

Figure 6. Schematic descriptions of the different blend morphologies in terms of polymer acceptor content. Reproduced under the terms of Attribution-NonCommercial-NoDerivatives 4.0 International license.[69] Copyright 2021 The Authors.

Polymer acceptors with good mechanical and electrical characteristics can be a promising option to improve the mechanical properties of active layer incorporating SMAs. NDI-based polymer acceptors with a high MW above the critical MW are easily accessible, which can form tie molecules and entangled chains in the active layer and contributes to high mechanical toughness and ductility. Kim et al.[69] incorporated high-MW P(NDI2OD-T2) into the PM6:Y7 blend to concurrently increase PCE and

stretchability (**Figure 6**). The P(NDI2OD-T2) featuring high MW above the critical MW improved charge transport and increases the PCE from 14.6% to 15.4%. Meanwhile, the addition of 10-20 wt% P(NDI2OD-T2) engendered a more than 4-fold increase in mechanical ductility. The ternary active layer showed ductile plastic deformation and considerable wrinkling, whereas the PM6:Y7 active layer formed a brittle break. The effectiveness of high-Mw polymer acceptors is that they provided electrical and mechanical bridges between adjacent SMA domains.

To improve the mechanical behavior of active layer, Chu et al. designed and utilized polymer donor, PBB1-Cl, as a third component.[70] PM6 and PBB1-Cl films had similar Rs values, indicating high compatibility between them. The strong planarity and low steric hindrance of PBB1-Cl facilitated intermolecular packing and entanglement in the active layer, engendering a 4.6-fold improvement in the tensile properties of active layer (5.83% vs. 26.86%). With PBB1-Cl, the PCE of the rigid device increased from 15.83% to 17.36%, and that of flexible device ascended from 13.44% to 14.96%. After 500 bending cycles with a radius of 5 mm, the flexible ternary OPVs based on PM6:Y6-BO-4Cl:PBB1-Cl still retained over 74% of the initial PCE.

4.3.4. D/A compatibilizer

D/A compatibilizers can reduce the interfacial tension between donor and acceptor phases and improve miscibility. Compatibilizers can provide kinetic barriers to prevent

excessive domain coalescence; compatibilizers can also increase the interfacial adhesion and cohesion characteristics of D/A heterojunctions.

Kim et al.[71] demonstrated the use of P3HT-g-P2VP as compatibilizer in OPVs, which efficaciously modified the sharp interface between fullerene derivatives and P3HT, and thereby improved mechanical stability without sacrificing PCE. The fracture energy of OPVs with 5% P3HT-g-P2VP was enhanced above 20% in relative to the control device. P3HT-g-P2VP exhibited a better compatibilizing effect than linear-type P3HT-b-P2VP, and the broad interfacial width and low interfacial tension due to the higher preferential segregation of P3HT-g-P2VP at the interface availably enhances the mechanical stabilities. They further reported another compatibilizer, an acceptor-donor-acceptor triad-type small molecule, 5TRh-PCBM,[72] which consisted of an oligothiophene segment and fullerene derivatives as the central core and end groups, respectively. The 5TRh core preferentially interacted with polymer donors bearing thiophene or fused-thiophene units, while the end fullerene groups was inclined to interact with PCBM. Unlike typical compatibilizers, 5TRh-PCBM improved PCEs due to its light-harvesting capability. The preferential localization of 5TRh-PCBM at the D/A interfaces modified the weak D/A interface, reduced the interfacial tension, and enhanced the resistance against crack growth and debonding between donor and acceptor domains. Therefore, the cohesive fracture energy (Gc) values of the PBDB-T:

$PC_{71}BM$ active layer increased from 1.06 ± 0.14 to 2.93 ± 0.15 J m^{-2} after the incorporation of 10 wt% 5TRh-PCBM. In their follow-up work, they reported the donor-acceptor alternating copolymer-type compatibilizer (PBDTY5-Cl), and introduced it into the PBDB-T: Y10-Br active layer.[42] The addition of PBDTY5-Cl availably reduced the D/A interfacial tensions and stabilized the D/A interfaces, preventing excessive coalescence of domains. The incorporation of 20 wt % PBDTY5-Cl endowed OPVs with a PCE of 17.1% and Gc of 0.89 J m^{-2}, higher than the binary counterpart (PCE of 13.6% and Gc of 0.35 J m^{-2}).

4.3.5. PCBM

It is difficult to realize high PCE and good mechanical stability simultaneously, as highly crystalline or aggregated microstructures, which are thought to be critical for efficient device operation, make the active layer stiff and brittle. The insertion of low-proportion fullerene acceptor into a non-fullerene binary blend promotes charge transport due to its high electron mobility, and improve charge separation and mechanical robustness by scattering into the amorphous region of the polymer matrix.

Someya et al.[73] prepared a 3-μm-thick ultra-flexible ternary OPV based on fullerene/non-fullerene acceptors with a high PCE of 13% and good mechanical stability in compression and bending. After the addition of $PC_{71}BM$ to the PBDTTT-OFT: IEICO-4F binary blend, both PBDTTT-OFT and IEICO-4F maintained their face-

on orientation, while the crystallinity of IEICO-4F decreased by approximately 30%. The intrinsic high electron mobility of $PC_{71}BM$ compensated for the lower crystallinity of IEICO-4F, indicated by the increase of electron mobility from 3.7×10^4 (binary blend) to 5.2×10^4 $cm^2V^{-1}s^{-1}$ (ternary blend). Due to the low proportion of $PC_{71}BM$, most $PC_{71}BM$ scattered into the amorphous region of the polymer matrix rather than form brittle $PC_{71}BM$ aggregates, which improved the mechanical property. 3-mm-thick ultra-flexible OPVs with fullerene/non-fullerene mixed acceptors attain a PCE of 13% with 97% PCE retention after 1,000 bending cycles with 0.5-mm bending radius and 89% PCE retention after 1,000 compression-stretching cycles (45% compression and bending radius of 10 μm) by forming a buckling device structure. Parallelly, Ge et al.[74] added $PC_{71}BM$ to the D18-Cl: Y6 system to create ultrathin and ultralightweight OPVs. The active layer attained its preferred face-on orientation with degraded crystallinity and exhibited higher electron mobility after the addition of $PC_{71}BM$. The ultrathin and ultra-lightweight OPVs displayed a stable PCE of 15.5% and a high power-per-weight of 32.07 W g^{-1} at a weight of 4.83 g m^{-2}. The ultra-flexible ternary OPVs exhibited PCE retention of over 83% after 800 compression–stretching cycles, compared with binary OPVs (76%).

5. Conclusions/perspective

Organic photovoltaics are a hot topic in materials science and will be a key new

technology for low-cost renewable energy generation. Many significant advancements have been made in almost every aspect of OPVs in recent decades, including materials design, device engineering, and large-scale production, engendering high PCEs of around 20%. With the promise of being flexible, mechanically robust, and conformable for applications, recent research began to focus on the optimization and characterization of the mechanical properties of OPVs, which are often disregarded in literature. This perspective first analyzes the static and dynamic working conditions of flexible OPVs, and provides three strategies towards mechanical robust active layer: improve ductility, strengthen D/A interface, and restrain molecule migration. This perspective highlights the most recent advances towards the development of mechanically robust OPVs in the aspects of all-polymer active layer, single-component active layer, and ternary component strategy. The following directions and endeavors are given for future flexible OPV development:

A. Control molecule pre-aggregation/entanglement in solution.[75] The aggregate state of active materials in prepared solution is critical for the morphology and mechanical properties of active layers. According to the theory of Flory and de Gennes, polymer solutions can be classified into three type based on polymer concentrations: (1) dilute solution, where the polymer concentration < the contact concentration (c*), and polymers don't contact or entangle; (2) semi-dilute solution, where polymer

concentration is between c* and the entanglement concentration (Ce), and polymers contact with each other but no entanglement occurs; (3) concentrated solution, in which the polymer concentration is higher than Ce, and polymers contact and entangle with each other. To facilitate polymers to contact and entangle at high concentration, the donor: acceptor solution can be prepared at a very high polymer concentration and then diluted to a low polymer concentration for spin-coating. The polymer aggregate state in solution can be maintained during dilution since the diffusion of solvent molecules into polymers is much quicker than the diffusion of polymers in solvent molecules. Entanglement of polymer chains is in favor of mechanical robust active layers.

B. Dynamic non-covalent interaction. High stretchability and self-healing qualities can be achieved by incorporating dynamic non-covalent bonds between flexible polymer chains. Apart from the stretching and alignment of polymer chains in the amorphous area and the break of crystalline domains, the dynamic bonds can readily be broken to allow energy dissipation upon strain, making the system more tolerant to strain and mechanical stimuli. This method does not dramatically affect the pi-conjugation compared with insertion of conjugation-breaking units in the conjugated backbone or insulating low Tg amorphous polymer side-chains, allowing for both good mechanical compliance and high charge mobility. Several works have proved the effectiveness of amide moieties in promoting mechanical robustness.[76-78] However,

it's worth noting that non-covalent bonding strength is not the sole predictor of mechanical performance. The impact of non-covalent bonding on crystalline packing has a considerable impact on performance, which may outweigh any gain afforded by hydrogen bond energy dissipation. Furthermore, due to the incorporation of dynamic bonding, the polymers have shown some healing capabilities by almost recovering their initial physical properties upon a mild healing treatment.

C. Controlling the regioregularity of conjugated polymers. High regioregularity (RR) conjugated polymers exhibit good optical and electrical properties but often induce but poor mechanical resilience, and vice versa for the low RR materials.[79] Therefore, precise RR control is important in the design of conjugated polymers for mechanically robust active layer. Both electrical and mechanical properties can be optimized simultaneously blending photoactive materials with high and low RR or combining high RR and low RR blocks in one polymer chain. A small amount of high RR materials in a low RR material matrix can produce mobilities that are similar to pure high RR materials while also increasing COS and toughness.

D. Fiber-reinforcement. In terms of mechanical performance, nanotube or nanowire-based materials can be employed as reinforcement materials in active layer, inspired by reinforcement wires in concrete. Randomly distributed nanofibers in the polymer matrix can improve toughness and slow crack growth. The density, orientation, and

porosity of nanofibers can be controlled to enhance flexibility/stretchability, while maintain the PCE of OPVs.

E. Sequential deposition. The brittle nature of small molecules in most high-efficiency OPVs encourages easy formation of cracks in the photoactive film under deformation. Sequential coating can be used to realize the rational control over vertical phase separation, to realize highly deformable while efficient OPVs.[80] The optimized morphology exhibits distinct donor-rich and homogenous region distributed along the vertical direction. The donor-rich zone provides sufficient chain entanglements and strong interfaces, which are helpful to mechanical durability, while the homogeneously mixed region produces a continuous interpenetrating network that allows for high device throughput.

Despite the progress, there are still many challenges to overcome in attempt to fabricate stretchable, mechanically robust, and conformable OPVs. First, new highly stretchable substrates, conductors, and interfaces should be developed in parallel with donors and acceptors. A quantitative relationship between mechanical energy and active layer should also be revealed. Finally, successful lab-to-manufacturing translation of flexible and mechanically robust OPVs is a major challenge.

Abbreviations

BTP-BO-4Cl

2,2'-((2Z,2'Z)-((12,13-bis(2-butyloctyl)-3,9-diundecyl-12,13-dihydro-[1,2,5]thiadiazolo[3,4-*e*]thieno[2",3":4',5']thieno[2',3':4,5]pyrrolo[3,2-*g*]thieno[2',3':4,5]thieno[3,2-*b*]indole-2,10-diyl)bis(methanylylidene))bis(5,6-dichloro-3-oxo-2,3-dihydro-1*H*-indene-2,1-diylidene))dimalononitrile

D18-Cl

Poly[(2,6-(4,8-bis(5-(2-ethylhexyl-3-chloro)thiophen-2-yl)-benzo[1,2-*b*:4,5-*b*']dithiophene))-alt-5,5'-(5,8-bis(4-(2-butyloctyl)thiophen-2-yl)dithieno[3',2':3,4;2",3":5,6]benzo[1,2-*c*][1,2,5]thiadiazole)]

N3

2,2'-((2Z,2'Z)-((12,13-bis(3-ethylheptyl)-3,9-diundecyl-12,13-dihydro [1,2,5]thiadiazolo[3,4-e]thieno[2",3":4',5']thieno[2',3':4,5]pyrrolo[3,2-g]thieno[2',3':4,5]thieno[3,2-*b*]indole-2,10-diyl)bis(methanylylidene))bis(5,6-difluoro-3-oxo-2,3-dihydro-1*H*-indene-2,1-diylidene))dimalononitrile

PBDTTTPD

Poly[(5,6-dihydro-5-octyl-4,6-dioxo-4*H*-thieno[3,4-*c*]pyrrole-1,3-diyl)[4,8-bis[5-(2-ethylhexyl)-2-thienyl]benzo[1,2-*b*:4,5-*b*']dithiophene-2,6-diyl]]

PTB7-Th

Poly[4,8-bis(5-(2-ethylhexyl)thiophen-2-yl)benzo[1,2-*b*;4,5-*b*']dithiophene-2,6-diyl-alt-(4-(2-ethylhexyl)-3-fluorothieno[3,4-*b*]thiophene-)-2-carboxylate-2-6-diyl)]

PTB7

Poly [[4,8-bis[(2-ethylhexyl)oxy]benzo[1,2-*b*:4,5-*b*']dithiophene-2,6-diyl][3-fluoro-2-[(2-ethylhexyl)carbonyl]thieno[3,4-*b*]thiophenediyl]]

PBDTTT-OFT

Poly[4,8-bis(5-(2-ethylhexyl)thiophen-2-yl)benzo[1,2-*b*;4,5-*b*']dithiophene-2,6-diyl-alt-(4-octyl-3-fluorothieno[3,4-b]thiophene)-2-carboxylate-2–6-diyl]

PBDB-T

Poly[(2,6-(4,8-bis(5-(2-ethylhexyl)thiophen-2-yl)-benzo[1,2-*b*:4,5-b']dithiophene))-alt-(5,5-(1',3'-di-2-thienyl-5',7'-bis(2-ethylhexyl)benzo[1',2'-*c*:4',5'-*c*']dithiophene-4,8-dione)]

PM6

Poly[(2,6-(4,8-bis(5-(2-ethylhexyl-3-fluoro)thiophen-2-yl)-benzo[1,2-*b*:4,5-*b*']dithiophene))-alt-(5,5-(1',3'-di-2-thienyl-5',7'-bis(2-ethylhexyl)benzo[1',2'-*c*:4',5'-*c*']dithiophene-4,8-dione)]

P3HT Poly(3-hexylthiophene)

Y6

2,2'-((2Z,2'Z)-((12,13-bis(2-ethylhexyl)-3,9-diundecyl-12,13-dihydro-[1,2,5]thiadiazolo[3,4-e]thieno[2",3":4',5']thieno[2',3':4,5]pyrrolo[3,2-

g]thieno[2',3':4,5]thieno[3,2-b]indole-2,10-diyl)bis(methanylylidene))bis(5,6-difluoro-3-oxo-2,3-dihydro-1H-indene-2,1-diylidene))dimalononitrile

Y7

2,2'-((2Z,2'Z)-((12,13-bis(2-ethylhexyl)-3,9-diundecyl-12,13-dihydro-[1,2,5]thiadiazolo[3,4-*e*]thieno[2",3":4',5']thieno[2',3':4,5]pyrrolo[3,2-*g*]thieno[2',3':4,5]thieno[3,2-*b*]indole-2,10-diyl)bis(methanylylidene))bis(5,6-dichloro-3-oxo-2,3-dihydro-1*H*-indene-2,1-diylidene))dimalononitrile

Y5-2BO

2,2'-((2Z,2'Z)-((12,13-bis(2-butyloctyl)-3,9-diundecyl-12,13-dihydro-[1,2,5]thiadiazolo[3,4-*e*]thieno[2",3":4',5']thieno[2',3':4,5] pyrrolo[3,2-*g*]thieno[2',3':4,5]thieno[3,2-*b*]indole-2,10-diyl)bis(methaneylylidene))bis(3-oxo-2,3-dihydro-1*H*-indene-2,1-diylidene))dimalononitrile

IEICO-4F

2,2'-((2Z,2'Z)-(((4,4,9,9-tetrakis(4-hexylphenyl)-4,9-dihydro-sindaceno[1,2-*b*:5,6-*b*']dithiophene-2,7-diyl)bis(4-((2-ethylhexyl)oxy)thiophene-5,2-diyl))bis(methanylylidene))bis(5,6-difluoro-3-oxo-2,3-dihydro-1*H*-indene-2,1-diylidene))dimalononitrile

$PC_{61}BM$

[6,6]-Phenyl-C61-butyric-acid-methyl-ester

$PC_{71}BM$

[6,6]-Phenyl-C71-butyric-acid-methyl-ester

OXCBA

o-xylenyl C60 bis-adduct

P3HT-b-P2VP

Poly(3-hexylthiophene)-block-poly(2-vinylpyridine)

P3HT-g-P2VP

Poly(3-hexylthiophene)-graft-poly(2-vinylpyridine)

PBDTY5-Cl

Poly(5,5-2,2'-((2Z,2'Z)-((12,13-bis(2-decyltetradecyl)-3,9-diundecyl-12,13-dihydro[1,2,5]thiadiazolo[3,4-e]thieno[2",3":4',5']thieno[2',3':4,5]pyrrolo[3,2-g]thieno[2',3':4,5]thieno[3,2-*b*]indole-2,10-diyl)-bis(methaneylylidene))bis(3-oxo-2,3-dihydro-1*H*-indene-2,1diylidene))dimalononitrile-alt-2,6-4,8-bis(4-chloro-5-(2-ethylhexyl)thiophen-2-yl)benzo[1,2-*b*:4,5-*b*']dithiophene)

PDMS

Poly(dimethylsiloxane)

PDPS

Poly(dimethylsiloxane-co-methylphenethyl-siloxane)

PEDOT:PSS

Poly(3,4-ethylenedioxythiophene):poly(styrene sulfonate)
P(NDI2OD)-T2
Poly[[N,N'-bis(2-octyldodecyl)naphthalene-1,4,5,8-bis(dicarboximide)-2,6-diyl]-alt-5,5'-(2,2'-bithiophene)]
SEBS
Polystyrene-block-poly(ethyleneran-butylene)-block-polystyrene
Y10-Br
2,2'-((2Z,2'Z)((12,13-bis(2-butyloctyl)-3,9-diundecyl-12,13-dihydro-[1,2,5]-thiadiazolo[3,4-*e*]thieno[2'',3'':4',5']thieno[2',3':4,5]pyrrolo[3,2-*g*]thieno[2',3':4,5]thieno[3,2-*b*]indole-2,10-diyl)bis(methanylylidene))bis(3-bromo-6-oxo-5,6-dihydro-4*H*-cyclopenta[*b*]thiophene-4-ylidene)dimalononitrile

Acknowledgements

This work is supported by the National Natural Science Foundation of China (Grant No. 51873127 and No. 22179087). G. Li thanks the Research Grants Council of Hong Kong (GRF grant 15218517, CRF C5037-18G, PDFS2021-5S04), National Natural Science Foundation of China (NSFC 51961165102), the funding support from Shenzhen Science and Technology Innovation Commission (Project No. JCYJ 20200109105003940), the Sir Sze-yuen Chung Endowed Professorship Fund (8-8480) provided by the Hong Kong Polytechnic University.

Conflict of Interest

The authors declare no conflict of interest

Received: ((will be filled in by the editorial staff))
Revised: ((will be filled in by the editorial staff))
Published online: ((will be filled in by the editorial staff))

References

[1] C. Yan, S. Barlow, Z. Wang, H. Yan, A. K. Y. Jen, S. R. Marder, X. Zhan, *Nat. Rev. Mater.* **2018**, *3*, 18003.

[2] G. Li, R. Zhu, Y. Yang, *Nat. Photon.* **2012**, *6*, 153.

[3] P. Cheng, G. Li, X. Zhan, Y. Yang, *Nat. Photon.* **2018**, *12*, 131.

[4] Y. Li, *Acc. Chem. Res.* **2012**, *45*, 723.

[5] C. Duan, K. Zhang, C. Zhong, F. Huang, Y. Cao, *Chem. Soc. Rev.* **2013**, *42*, 9071.

[6] Y. Chen, X. Wan, G. Long, *Acc. Chem. Res.* **2013**, *46*, 2645.

[7] H. Yao, L. Ye, H. Zhang, S. Li, S. Zhang, J. Hou, *Chem. Rev.* **2016**, *116*, 7397.

[8] C. J. Brabec, M. Heeney, I. McCulloch, J. Nelson, *Chem. Soc. Rev.* **2011**, *40*, 1185.

[9] H. Hu, P. C. Y. Chow, G. Zhang, T. Ma, J. Liu, G. Yang, H. Yan, *Acc. Chem. Res.* **2017**, *50*, 2519.

[10] P. Cheng, Y. Yang, *Acc. Chem. Res.* **2020**, *53*, 1218.

[11] Z. Zheng, J. Wang, P. Bi, J. Ren, Y. Wang, Y. Yang, X. Liu, S. Zhang, J. Hou, *Joule* **2022**, *6*, 171.

[12] C. Li, J. Zhou, J. Song, J. Xu, H. Zhang, X. Zhang, J. Guo, L. Zhu, D. Wei, G. Han, J. Min, Y. Zhang, Z. Xie, Y. Yi, H. Yan, F. Gao, F. Liu, Y. Sun, *Nat. Energy* **2021**, *6*, 605.

[13] L. Zhan, S. Li, Y. Li, R. Sun, J. Min, Z. Bi, W. Ma, Z. Chen, G. Zhou, H. Zhu, M. Shi, L. Zuo, H. Chen, *Joule* **2022**, DOI：10.1016/j.joule.2022.02.001.

[14] Y. Cui, Y. Xu, H. Yao, P. Bi, L. Hong, J. Zhang, Y. Zu, T. Zhang, J. Qin, J. Ren, Z. Chen, C. He, X. Hao, Z. Wei, J. Hou, *Adv. Mater.* **2021**, *33*, 2102420.

[15] F. Zhao, H. Zhang, R. Zhang, J. Yuan, D. He, Y. Zou, F. Gao, *Adv. Energy Mater.* **2020**, *10*, 2002746.

[16] P. Cheng, X. Zhan, *Chem. Soc. Rev.* **2016**, *45*, 2544.

[17] L. Duan, A. Uddin, *Adv. Sci.* **2020**, *7*, 1903259.

[18] W. Yang, W. Wang, Y. Wang, R. Sun, J. Guo, H. Li, M. Shi, J. Guo, Y. Wu, T. Wang, *Joule* **2021**, *5*, 1209.

[19] K. Zhou, J. Xin, W. Ma, *ACS Energy Lett.* **2019**, *4*, 447.

[20] X. Du, T. Heumueller, W. Gruber, A. Classen, T. Unruh, N. Li, C. J. Brabec,

Joule **2019**, *3*, 215.
[21] R. Søndergaard, M. Hösel, D. Angmo, T. T. Larsen-Olsen, F. C. Krebs, *Mater. Today* **2012**, *15*, 36.
[22] S. Savagatrup, A. D. Printz, T. F. O'Connor, A. V. Zaretski, D. Rodriquez, E. J. Sawyer, K. M. Rajan, R. I. Acosta, S. E. Root, D. J. Lipomi, *Energy Environ. Sci.* **2015**, *8*, 55.
[23] K. Fukuda, K. Yu, T. Someya, *Adv. Energy Mater.* **2020**, *10*, 2000765.
[24] Y. Sun, T. Liu, Y. Kan, K. Gao, B. Tang, Y. Li, *Small Sci.* **2021**, *1*, 2100001.
[25] Y. Li, G. Xu, C. Cui, Y. Li, *Adv. Energy Mater.* **2018**, *8*, 1701791.
[26] X. Chen, G. Xu, G. Zeng, H. Gu, H. Chen, H. Xu, H. Yao, Y. Li, J. Hou, Y. Li, *Adv. Mater.* **2020**, *32*, 1908478.
[27] W. Pan, Y. Han, Z. Wang, Q. Luo, C. Ma, L. Ding, *J. Semicond.* **2021**, *42*, 050301.
[28] Y. Sun, M. Chang, L. Meng, X. Wan, H. Gao, Y. Zhang, K. Zhao, Z. Sun, C. Li, S. Liu, H. Wang, J. Liang, Y. Chen, *Nat. Electron.* **2019**, *2*, 513.
[29] X. Meng, L. Zhang, Y. Xie, X. Hu, Z. Xing, Z. Huang, C. Liu, L. Tan, W. Zhou, Y. Sun, W. Ma, Y. Chen, *Adv. Mater.* **2019**, *31*, 1970294.
[30] W. Song, B. Fanady, R. Peng, L. Hong, L. Wu, W. Zhang, T. Yan, T. Wu, S. Chen, Z. Ge, *Adv. Energy Mater.* **2020**, *10*, 2000136.
[31] S. E. Root, S. Savagatrup, A. D. Printz, D. Rodriquez, D. J. Lipomi, *Chem. Rev.* **2017**, *117*, 6467.
[32] C. Liu, C. Xiao, C. Xie, W. Li, *Nano Energy* **2021**, *89*, 106399.
[33] J. Qin, L. Lan, S. Chen, F. Huang, H. Shi, W. Chen, H. Xia, K. Sun, C. Yang, *Adv. Funct. Mater.* **2020**, *30*, 2002529.
[34] H. Jinno, K. Fukuda, X. Xu, S. Park, Y. Suzuki, M. Koizumi, T. Yokota, I. Osaka, K. Takimiya, T. Someya, *Nat. Energy* **2017**, *2*, 780.
[35] X. Xu, K. Fukuda, A. Karki, S. Park, H. Kimura, H. Jinno, N. Watanabe, S. Yamamoto, S. Shimomura, D. Kitazawa, T. Yokota, S. Umezu, T.-Q. Nguyen, T. Someya, *Proc. Natl. Acad. Sci. U.S.A.* **2018**, *115*, 4589.
[36] Y. Cao, P. Smith, A. J. Heeger, *Polymer* **1991**, *32*, 1210.
[37] B. O'Connor, R. J. Kline, B. R. Conrad, L. J. Richter, D. Gundlach, M. F. Toney, D. M. DeLongchamp, *Adv. Funct. Mater.* **2011**, *21*, 3697.
[38] L. Li, J. Liang, H. Gao, Y. Li, X. Niu, X. Zhu, Y. Xiong, Q. Pei, *ACS Appl. Mater. Inter.* **2017**, *9*, 40523.
[39] P. B. J. St Onge, M. U. Ocheje, M. Selivanova, S. Rondeau-Gagne, *Chem. Rec.* **2019**, *19*, 1008.
[40] C. Lee, S. Lee, G.-U. Kim, W. Lee, B. J. Kim, *Chem. Rev.* **2019**, *119*, 8028.
[41] C. C. Xie, X. D. Jiang, Q. L. Zhu, D. Wang, C. Y. Xiao, C. H. Liu, W. Ma, Q.

M. Chen, W. W. Li, *Small Methods* **2021**, *5*, 2100481.
[42] J.-W. Lee, C. Sun, D. J. Kim, M. Y. Ha, D. Han, J. S. Park, C. Wang, W. B. Lee, S.-K. Kwon, T.-S. Kim, Y.-H. Kim, B. J. Kim, *ACS Nano* **2021**, *15*, 19970.
[43] H. Sun, X. Guo, A. Facchetti, *Chem* **2020**, *6*, 1310.
[44] A. Facchetti, *Mater. Today* **2013**, *16*, 123.
[45] K. Zhang, R. Xia, B. Fan, X. Liu, Z. Wang, S. Dong, H.-L. Yip, L. Ying, F. Huang, Y. Cao, *Adv. Mater.* **2018**, *30*, 1803166.
[46] P. Cheng, X. Zhao, X. Zhan, *Acc. Mater. Res.* **2022**, *3*, 309.
[47] Y. Meng, J. Wu, X. Guo, W. Su, L. Zhu, J. Fang, Z.-G. Zhang, F. Liu, M. Zhang, T. P. Russell, *Sci. China Chem.* **2019**, *62*, 845.
[48] T. Kim, J. H. Kim, T. E. Kang, C. Lee, H. Kang, M. Shin, C. Wang, B. W. Ma, U. Jeong, T. S. Kim, B. J. Kim, *Nat. Commun.* **2015**, *6*, 8547.
[49] N. Balar, J. J. Rech, R. Henry, L. Ye, H. Ade, W. You, B. T. O'Connor, *Chem. Mater.* **2019**, *31*, 5124.
[50] J.-W. Lee, B. S. Ma, J. Choi, J. Lee, S. Lee, K. Liao, W. Lee, T.-S. Kim, B. J. Kim, *Chem. Mater.* **2020**, *32*, 582.
[51] Z. G. Zhang, Y. Li, *Angew. Chem. Int. Ed.* **2021**, *60*, 4422.
[52] Q. Fan, W. Su, S. Chen, W. Kim, X. Chen, B. Lee, T. Liu, U. A. Méndez-Romero, R. Ma, T. Yang, W. Zhuang, Y. Li, Y. Li, T.-S. Kim, L. Hou, C. Yang, H. Yan, D. Yu, E. Wang, *Joule* **2020**, *4*, 658.
[53] J.-W. Lee, C. Sun, B. S. Ma, H. J. Kim, C. Wang, J. M. Ryu, C. Lim, T.-S. Kim, Y.-H. Kim, S.-K. Kwon, B. J. Kim, *Adv. Energy Mater.* **2021**, *11*, 2003367.
[54] S. Liang, X. Jiang, C. Xiao, C. Li, Q. Chen, W. Li, *Acc. Chem. Res.* **2021**, *54*, 2227.
[55] Y. He, T. Heumüller, W. Lai, G. Feng, A. Classen, X. Du, C. Liu, W. Li, N. Li, C. J. Brabec, *Adv. Energy Mater.* **2019**, *9*, 1900409.
[56] X. Jiang, J. Yang, S. Karuthedath, J. Li, W. Lai, C. Li, C. Xiao, L. Ye, Z. Ma, Z. Tang, F. Laquai, W. Li, *Angew. Chem. Int. Ed.* **2020**, *59*, 21683.
[57] G. Feng, J. Li, Y. He, W. Zheng, J. Wang, C. Li, Z. Tang, A. Osvet, N. Li, C. J. Brabec, Y. Yi, H. Yan, W. Li, *Joule* **2019**, *3*, 1765.
[58] G. Feng, J. Li, F. J. M. Colberts, M. Li, J. Zhang, F. Yang, Y. Jin, F. Zhang, R. A. J. Janssen, C. Li, W. Li, *Journal of the American Chemical Society* **2017**, *139*, 18647.
[59] G. Feng, W. Tan, S. Karuthedath, C. Li, X. Jiao, A. C. Y. Liu, H. Venugopal, Z. Tang, L. Ye, F. Laquai, C. R. McNeill, W. Li, *Angew. Chem. Int. Ed.* **2021**, *60*, 25499.
[60] C. Xie, C. Xiao, X. Jiang, S. Liang, C. Liu, Z. Zhang, Q. Chen, W. Li, *Macromolecules* **2022**, *55*, 322.
[61] Z. Y. Wang, M. C. Xu, Z. L. Li, Y. R. Gao, L. Yang, D. Zhang, M. Shao, *Adv. Funct. Mater.* **2021**, *31*, 2103534.

[62] S. Chen, S. Jung, H. J. Cho, N.-H. Kim, S. Jung, J. Xu, J. Oh, Y. Cho, H. Kim, B. Lee, Y. An, C. Zhang, M. Xiao, H. Ki, Z.-G. Zhang, J.-Y. Kim, Y. Li, H. Park, C. Yang, *Angew. Chem. Int. Ed.* **2018**, *57*, 13277.
[63] M. Prete, E. Ogliani, M. Bregnhoj, J. S. Lissau, S. Dastidar, H. G. Rubahn, S. Engmann, A. L. Skov, M. A. Brook, P. R. Ogilby, A. Printz, V. Turkovic, M. Madsen, *J. Mater. Chem. C* **2021**, *9*, 11838.
[64] Z. Peng, K. Xian, Y. Cui, Q. Qi, J. Liu, Y. Xu, Y. Chai, C. Yang, J. Hou, Y. Geng, L. Ye, *Adv. Mater.* **2021**, *33*, 2106732.
[65] J. Han, F. Bao, X. Wang, D. Huang, R. Yang, C. Yang, X. Jian, J. Wang, X. Bao, J. Chu, *Cell Rep. Phys. Sci.* **2021**, *2*, 100408.
[66] Y. Wang, J. Lee, X. Hou, C. Labanti, J. Yan, E. Mazzolini, A. Parhar, J. Nelson, J.-S. Kim, Z. Li, *Adv. Energy Mater.* **2021**, *11*, 2003002.
[67] J. Han, F. Bao, D. Huang, X. Wang, C. Yang, R. Yang, X. Jian, J. Wang, X. Bao, J. Chu, *Adv. Funct. Mater.* **2020**, *30*, 2003654.
[68] J. W. Mok, Z. Q. Hu, C. X. Sun, I. Barth, R. Munoz, J. Jackson, T. Terlier, K. G. Yager, R. Verduzco, *Chem. Mater.* **2018**, *30*, 8314.
[69] J.-W. Lee, B. S. Ma, H. J. Kim, T.-S. Kim, B. J. Kim, *JACS Au* **2021**, *1*, 612.
[70] J. Wang, C. Han, F. Bi, D. Huang, Y. Wu, Y. Li, S. Wen, L. Han, C. Yang, X. Bao, J. Chu, *Energy Environ. Sci.* **2021**, *14*, 5968.
[71] H. J. Kim, J.-H. Kim, J.-H. Ryu, Y. Kim, H. Kang, W. B. Lee, T.-S. Kim, B. J. Kim, *ACS Nano* **2014**, *8*, 10461.
[72] G.-U. Kim, Y. W. Lee, B. S. Ma, J. Kim, J. S. Park, S. Lee, T. L. Nguyen, M. Song, T.-S. Kim, H. Y. Woo, B. J. Kim, *J. Mater. Chem. A* **2020**, *8*, 13522.
[73] W. Huang, Z. Jiang, K. Fukuda, X. Jiao, C. R. McNeill, T. Yokota, T. Someya, *Joule* **2020**, *4*, 128.
[74] W. Song, K. Yu, E. Zhou, L. Xie, L. Hong, J. Ge, J. Zhang, X. Zhang, R. Peng, Z. Ge, *Adv. Funct. Mater.* **2021**, *31*, 2102694.
[75] P. Cheng, C. Yan, Y. Li, W. Ma, X. Zhan, *Energy Environ. Sci.* **2015**, *8*, 2357.
[76] J. Y. Oh, S. Rondeau-Gagné, Y.-C. Chiu, A. Chortos, F. Lissel, G.-J. N. Wang, B. C. Schroeder, T. Kurosawa, J. Lopez, T. Katsumata, J. Xu, C. Zhu, X. Gu, W.-G. Bae, Y. Kim, L. Jin, J. W. Chung, J. B. H. Tok, Z. Bao, *Nature* **2016**, *539*, 411.
[77] M. U. Ocheje, M. Selivanova, S. Zhang, T. H. Van Nguyen, B. P. Charron, C.-H. Chuang, Y.-H. Cheng, B. Billet, S. Noori, Y.-C. Chiu, X. Gu, S. Rondeau-Gagné, *Polymer Chemistry* **2018**, *9*, 5531.
[78] L. A. Galuska, M. U. Ocheje, Z. C. Ahmad, S. Rondeau-Gagné, X. Gu, *Chem. Mater.* **2022**, *34*, 2259.
[79] Y. Kim, H. Park, J. S. Park, J.-W. Lee, F. S. Kim, H. J. Kim, B. J. Kim, *J. Mater. Chem. A* **2022**, *10*, 2672.

[80] Q. Zhu, J. Xue, G. Lu, B. Lin, H. B. Naveed, Z. Bi, G. Lu, W. Ma, *Nano Energy* **2022**, *97*, 107194.

Table l Mechanical properties of active layers and related device performance of OPVs.

Active layer	Tensile Modulus [GPa]	Toughness [MJ m^{-3}]	Cohesive fracture energy [J m^{-2}]	Tensile Strength [MPa]	Crack onset strain [%]	V_{OC}[a] [V]	J_{SC}[a] [mA cm^{-2}]	FF[a]	PCE[a] [%]	Ref.
PBDTTTPD:P(NDI2HD-T)		5.687×10^{-4}			7.16	1.06 (1.062±0.001)	11.22 (11.243±0.028)	0.56 (0.553±0.006)	6.64 (6.601±0.058)	[48]
PBDTTTPD:$PC_{61}BM$		3.4×10^{-6}			0.30	0.96 (0.959±0.003)	11.17 (11.208±0.057)	0.57 (0.565±0.007)	6.12 (6.076±0.045)	[48]
PM6:PF2-DTC	0.99±0.14	14.35±1.36		17.3±1.1	11.3±0.6	0.97	14.11	0.608	8.31	[52]
PM6:PF2-DTSi	0.72±0.11	9.30±0.09		15.5±0.6	8.6±1.6	0.99	16.48	0.661	10.77	[52]
PM6:PF2-DTGe	0.79±0.11	7.33±1.80		15.7±0.7	6.7±1.2	0.97	14.48	0.576	8.09	[52]
PM6:IDIC16	1.03±0.16	0.82±0.52		10.4±2.2	1.4±0.4	0.98	10.96	0.457	4.93	[52]
PBDB-T:Y5-2BO	1.48±0.09	0.32±0.15			2.28±0.48	(0.89±0.00)	(13.04±0.11)	(0.60±0.01)	7.02(6.91±0.09)	[53]
PBDB-T: P(BDT2BOY5-H)	0.75±0.05	3.80±0.37			19.27±0.26	(0.92±0.01)	(18.61±0.17)	(0.51±0.02)	8.81(8.65±0.14)	[53]
PBDB-T: P(BDT2BOY5-F)	0.90±0.04	3.51±0.02			16.71±0.26	(0.92±0.01)	(19.03±0.23)	(0.55±0.01)	9.83(9.64±0.15)	[53]
PBDB-T: P(BDT2BOY5-Cl)	0.82±0.03	3.24±0.33			15.89±0.89	(0.92±0.01)	(18.72 ± 0.24)	(0.63 ± 0.02)	11.12(10.67±0.17)	[53]
JP02 (AgNWs/PET)	1.72	8.645×1			3.12	0.925	10.93	0.7121	7.21	[41]

		0^{-5}				(0.91±0.008)	(11.28±0.27)	(0.6924±0.0148)	(7.12±0.06)	
JP02 (ITO/Glass)						0.945 (0.942±0.005)	12.63 (12.21±0.62)	0.6724 (0.6543±0.0229)	8.02 (7.52±0.34)	[41]
PTB7-Th:IEICO-4F						0.70	25.0	0.646	11.4	[61]
PTB7-Th:IEICO-4F:5% PDMS						0.69	24.6	0.637	10.8	[61]
TQ-F:N2200	0.75	6.90		24.97	32.56	0.841 (0.840±0.001)	13.58 (13.52±0.18)	0.6233 (0.6182±0.83)	7.12 (7.02±0.14)	[62]
TQ-F:N2200:10% PDPS	0.54	9.67		24.62	50.92	0.840 (0.840±0.002)	12.40 (12.33±0.16)	0.6596 (0.6542±0.67)	6.87 (6.77±0.12)	[62]
PTB7:$PC_{71}BM$	2.19±0.37		1.32±0.40			0.72±0.01	13.1±0.4	0.697±0.046	6.6±0.5	[63]
PTB7:$PC_{71}BM$:3% AX	1.27±0.29		2.03±0.57			0.70±0.04	10.6±0.7	0.600±0.05	4.5±0.6	[63]
PTB7:$PC_{71}BM$:1.5% PDMS	1.98±0.44		1.38±0.52			0.73±0.01	13.0±0.2	0.671±0.05	6.3±0.4	[63]
PTB7:$PC_{71}BM$:3% AX:1.5% PDMS	2.36±0.22		1.42±0.35			0.68±0.01	9.8±0.1	0.646±0.022	4.3±0.2	[63]
PTB7:$PC_{71}BM$: 0.3% AXcPDMS	1.36±0.50		0.30±0.14			0.73±0.01	12.1±0.2	0.698±0.023	6.1±0.3	[63]
PTB7:$PC_{71}BM$: 0.03% AXcPDMS	1.39±0.28		1.15±0.36			0.70±0.03	12.5±0.5	0.691±0.035	6.1±0.5	[63]
PM6:N3	1.07±0.04				6.9±0.4	0.830 (0.834±0.004)	25.87 (25.70±0.3)	0.718 (0.717±0.005)	15.42 (15.37±0.14)	[64]
PM6:N3:2% SEBS	0.98±0.12				8.1±1.0	0.843	25.69	0.738	15.98	[64]

						(0.839±0.003)	(25.80±0.18)	(0.724±0.010)	(15.69±0.22)	
PM6:N3:5%SEBS	0.93±0.10				9.5±0.5	0.836 (0.839±0.003)	25.94 (25.71±0.10)	0.718 (0.709±0.007)	15.57 (15.28±0.20)	[64]
PM6:N3:10%SEBS	0.77±0.10				11.2±0.8	0.845 (0.839±0.002)	24.59 (24.62±0.10)	0.694 (0.686±0.003)	14.42 (14.17±0.11)	[64]
PM6:N3:20% SEBS	0.56±0.08				11.9±0.4	0.839 (0.840±0.002)	24.43 (24.18±0.12)	0.639 (0.631±0.005)	13.10 (12.81±0.15)	[64]
PM6:N3:30% SEBS	0.28±0.09				13.0±1.1	0.838 (0.839±0.003)	22.48 (22.33±0.08)	0.613 (0.605±0.004)	11.55 (11.34±0.09)	[64]
PM6:Y6					5.75	0.87 (0.87±0.01)	25.12 (25.17±0.5)	0.7057 (0.6895±0.0164)	15.44 (15.02±0.21)	[67]
PM6:Y6:30% PAEF					25.07	0.80 (0.81±0.01)	26.34 (26.23±0.32)	0.7168 (0.6934±0.0169)	15.17 (14.67±0.51)	[67]
PM6:Y7	1.60±0.29	0.31±0.05			2.21±0.22	0.86±0.01	24.27±0.19	0.69±0.01	14.62 (14.43±0.16)	[69]
PM6:Y7:10%P(NDI2OD-T2)	1.55±0.09	1.29±0.35			5.58±1.02	0.87±0.01	25.31±0.20	0.69±0.02	15.44 (15.19±0.21)	[69]
PM6:Y7:20%P(NDI2OD-T2)	1.63±0.09	2.76±0.24			10.02±0.94	0.87±0.01	25.74±0.18	0.67±0.01	15.01 (14.86±0.17)	[69]
PM6:Y7:30%P(NDI2OD-T2)	1.85±0.12	3.76±0.55			11.93±0.31	0.87±0.01	24.41±0.27	0.64±0.02	14.08 (13.68±0.28)	[69]
PM6:Y7:40%P(NDI2OD-T2)	1.51±0.09	4.74±0.38			16.56±0.44	0.87±0.01	23.52±0.20	0.58±0.01	11.91 (11.35±0.21)	[69]

PM6:Y7:50%P(NDI2OD-T2)	1.28±0.09	5.15±0.19			19.97±0.57	0.87±0.01	21.73±0.36	0.44±0.03	8.70 (8.36±0.33)	[69]
PM6:Y6-BO-4Cl					5.83	0.845	25.68	0.7294	15.83	[70]
PM6:Y6-BO-4Cl: 20% PBB1-Cl					26.86	0.866	26.84	0.7463	17.36	[70]
P3HT:OXCBA			4.51±0.11			0.87	9.30	0.61	4.94	[71]
P3HT:OXCBA: 5% P3HT-g-P2VP			5.46±0.42			0.89	9.28	0.63	5.21	[71]
P3HT:OXCBA: 5% P3HT-b-P2VP			4.75±0.20			0.89	9.30	0.61	5.11	[71]
PBDB-T:$PC_{71}BM$			1.06±0.14			0.85±0.01	12.69±0.08	0.67±0.01	7.39 (7.33±0.09)	[72]
PBDB-T:$PC_{71}BM$: 10% 5TRh-PCBM			2.93±0.15			0.86±0.01	13.01±0.19	0.64±0.01	7.25 (7.14±0.09)	[72]
PBDB-T:Y10-Br			0.35			0.93±0.01	22.18±0.24	0.66 ± 0.01	13.61 (13.34±0.18)	[42]
PBDB-T:Y10-Br:10% PBDTY5-Cl			0.62			0.92±0.00	22.84±0.17	0.70±0.01	14.70 (14.58±0.14)	[42]
PBDB-T:Y10-Br:20% PBDTY5-Cl			0.89			0.92±0.01	24.11±0.15	0.77±0.00	17.08 (16.80±0.12)	[42]
PBDTTT-OFT:IEICO-4F						0.71	24.7	0.68	11.9	[73]
PBDTTT-OFT:IEICO-4F:$PC_{71}BM$						0.72	26.1	0.69	13.0	[73]
D18-Cl:Y6						0.873	26.38	0.7692	17.72	[74]
D18-Cl:Y6:$PC_{71}BM$						0.860	27.04	0.7767	18.06	[74]

[a] Average data are in the brackets.

Biographical Information

Cenqi Yan is a postdoctoral research scholar in Prof. Gang Li's group in the Department of Electronic and Information Engineering, The Hong Kong Polytechnic University. Her current research focuses on organic solar cells. She received her B.S. degree in material physics from Shandong University (2013) and her Ph.D. degree in mechanics (advanced materials and mechanics) from Peking University (2018).

Gang Li is Sir Sze-yuen Chung Endowed Professor in renewable energy in the Department of Electronic and Information Engineering, associate director of Research Institute of Smart Energy (RISE) in the Hong Kong Polytechnic University. He obtained his B.S. degree from Wuhan University (China), M.S. and Ph.D. from Iowa State University (US),

respectively. His research interests are materials, device engineering, and device physics in organic semiconductors and hybrid perovskite semiconductors, focusing on energy applications. He is a Fellow of the Royal Society of Chemistry (RSC), the International Society for Optics and Photonic (SPIE), and Optica.

Pei Cheng received his B.E. in Polymer Materials and Engineering from Sichuan University in 2011. He then joined Prof. Xiaowei Zhan's group at Institute of Chemistry, Chinese Academy of Sciences (ICCAS)/Peking University, and received his Ph.D. in Chemistry (2016). Dr. Cheng worked in Prof. Yang Yang's group in Department of Materials Science and Engineering at University of California, Los Angeles from 2017 to 2020 as a Postdoc Researcher. He is currently a professor at Sichuan University. His research interests are focused on organic solar cells and functional optoelectronic devices.

The table of contents

Realizing a mechanically robust active layer is the key to enhancing the mechanical stability of organic photovoltaics (OPVs). This perspective analyses flexible OPV working conditions, summarizes recent strategies and achievements, and offers outlook and perspective for mechanically robust active layers.

Keywords: Solar cell

Cenqi Yan, Jiaqiang Qin, Yinghan Wang, Gang Li* and Pei Cheng*

Emerging Strategies toward Mechanically Robust Organic Photovoltaics: Focus on Active Layer